Heliyon 5 (2019) e02872

Contents lists available at ScienceDirect

Heliyon

journal homepage: www.heliyon.com

Research article

Rhodamine B dye sequestration using *Gmelina aborea* leaf powder

Olugbenga Solomon Bello [a,b,*], Esther Oluwadamilola Alabi [a], Kayode Adesina Adegoke [c], Samuel Adewale Adegboyega [a], Adejumoke Abosede Inyinbor [b], Adewumi Oluwasogo Dada [b]

[a] Department of Pure and Applied Chemistry, Ladoke Akintola University of Technology, P.M.B 4000, Ogbomoso, Oyo State, Nigeria
[b] Department of Physical Sciences, Industrial Chemistry Programme, Landmark University, Omu-Aran, Nigeria
[c] Department of Chemistry, University of Pretoria, Pretoria, 0002, South Africa

ARTICLE INFO

Keywords:
Biochemistry
Environmental science
Analytical chemistry
Surface chemistry
Rhodamine B dye
Kinetics
Gmelina arborea leaf
Isotherms

ABSTRACT

Chemically prepared activated carbon derived from *Gmelina aborea* leaves (GALAC) were used as adsorbent for the removal of Rhodamine B (Rh–B) dye from aqueous solutions. The adsorptive characteristics of activated carbon (AC) prepared from *Gmelina aborea* leaves (GAL) were studied using SEM, FTIR, pH point of zero charge (pH_{pzc}) and Boehm Titration (BT) techniques respectively. The effects of pH, contact time, initial dye concentration and solution temperature were also examined. Experimental data were analyzed using four different isotherm models: Langmuir, Freundlich, Temkin and Dubinin-Radushkevich. Four adsorption kinetic models: Pseudo-first-order (PFO), Pseudo-second-order (PSO), Elovich and Intraparticle diffusion models to establish the kinetics of adsorption process. The RhB dye adsorption on GALAC was best described by Langmuir isotherm model with maximum monolayer coverage of 1000 mg g^{-1} and R^2 value of 0. 9999. The EDX analysis revealed that GALAC contained 82.81% by weight and 91.2% by atom of carbon contents which are requisites for high adsorption capacity. Adsorption kinetic data best fitted the PSO kinetic model. Thermodynamic parameters obtained for GALAC are (ΔG^o ranged from -22.71 to -18.19 $kJmol^{-1}$; ΔH^o: 1.51 $kJmol^{-1}$; and ΔS^o: 0.39 $kJmol^{-1}$ K^{-1}respectively) indicating that the RhB dye removal from aqueous solutions by GALAC was spontaneous and endothermic in nature. The cost analysis established that GALAC is approximately eleven times cheaper than CAC thereby providing a saving of 351.41USD/kg. Chemically treated GAL was found to be an effective absorbent for the removal of RhB dye from aqueous solution.

1. Introduction

Pollution emanating from dye effluents has become a serious environmental problem in the last decade owing to the increasing and fast growing usage of dyes in different applications. Some dyes are resistance to fading even on exposing to light, water and various chemicals [1, 2, 3]. Dyes are chemically and/or thermally stable. Discharging dye effluents into the rivers or aqueous solutions is very dangerous because of the toxicity of such compounds to the living organism. Majority of contaminants (both dyes and chemical substances) present in aqueous solutions are from dye industries and manufacturing processes [3]. Dyes even at very low concentration(s) have negative influence on aquatic lives and food web. Ingestion of these dyes even at low concentration in aqueous media results in severe health complications that affect the central nervous system, reproductive system, brain and liver. In some cases they are mutagenic and carcinogenic [4, 5, 6, 7, 8]. Therefore, due to their harmful effects to both human and aquatic life, the removal of these colors from aqueous effluents become problematic because it poses a serious ecological damage due to its ability to extend to agricultural farm lands and water bodies. Therefore, dye effluents should not be directly discharge into the water bodies [1, 3, 9, 10, 11]. The treatment of dyes becomes imperative since a concentration as low as 1.0 mg/L in drinking water can impart intense color to the water and make it unsuitable for human consumption [3].

Over the years, applications of dyes in different industries including paper, textile, printing, plastics, food, rubber, etc have raised global concerns due to increasing contaminations to the ecosystems thereby raising issues to public health. The discharges of the effluents produced from these industries have detrimental consequences to aquatic life and humans [12, 13, 14, 15]. Also large volumes of water are required by textile industries in their operations, which in turn lead to the release of large volumes of effluents [3,4]. The distinctiveness in the composition of wastewater(s) from textile industries are such that they non-biodegradable and containing numerous dye materials [1, 4, 6, 16,

* Corresponding author.
E-mail address: osbello@lautech.edu.ng (O.S. Bello).

https://doi.org/10.1016/j.heliyon.2019.e02872
Received 11 October 2018; Received in revised form 1 November 2019; Accepted 14 November 2019

17]. This makes treatment of contaminated water demanding, since the colour tends to reoccur even after the removal process using conventional methods [18, 19, 20, 21, 22].

Numerous procedures for treating dye effluents include adsorption, coagulation, flocculation, oxidation, precipitation, electrolysis, reverse osmosis, liquid membrane separation, etc. By comparison, all these methods except adsorption have some inherent restrictions and drawbacks likes high operating cost, generation of by-products which are extremely hazardous, energy required is drastically intensive. Dyes are very stable to light and heat as well as have complex polymeric structures, thus making the biological method less flourishing or successful. Therefore ACs has become known as the only promising alternative to these conventional technologies in dyes and wastewaters treatment techniques. Based on this, among all physical techniques available, adsorption have been remains the superior method for treating both wastewater aqueous solution owing to its simplicity of design, lower cost, ease of operations, re-usability and insensitivities to toxicants [23]. Adsorption process has been confirmed as one of the prevalence wastewater treatment technologies in the world, making use of wide number of adsorbents [24, 25, 26].

However, in view of the low cost, regeneration potential and high adsorption capacity, agricultural wastes have been employed [3,24, 25, 26]. Various researchers have exploited adsorbents such as ackee apple (Blighia sapida) seeds [15], oil palm fruit [7,17,27], *Imperata cylindrical* [28], durian seed [29, 30] watermelon rinds [31], lime peel [32], Okra [33], fly ash [34, 35, 36], banana stalk [37, 38], etc for this purpose. A capable approach is increasing the adsorbents' porosity sites for enhancement of interactions between adsorbents and dyes. Recently, many researchers have looked into modifying the surface of adsorbents for total or complete removal of various dyes from the aqueous solution and generally reported that modifying agents increase the adsorption site(s) for both cationic and anionic dyes. Examples includes: guava leaf [39] bamboo [40, 41], plant leaf [42], coconut leaves [43, 44], kola nut and bean husk [45, 46], ficus racemosa [47, 48], Prunus Dulcis [49], durian Leaf [50], dead Leaves of plane trees [51], prunus dulcis [49], Moringa oleifera leaf [52, 53], C. camphora leaves [54], berry leaves [55], Glossogyne tenuifolia leaves [56]. Several authors have demonstrated the peculiarity of agricultural-based materials to remove various dyes having diverse molecular structures. Nevertheless, fabricating structures of such kinds of functionalized cellulosic adsorbents for efficient dyes removal remains a hot topic of consideration globally.

Gmelina aborea leaf is an agricultural waste, ubiquitously available all through the year at a no cost. *Gmelina aborea* grows on various localities and most especially on moist fertile valley. *Gmelina aborea* is a rapid growing tree which attains moderate to large height up to 40 m and 140 cm in diameter [57]. It occurs naturally in major part of India at altitudes up to 1,500 m and naturally in Thailand, Cambodia, Myanmar, Vietnam, Laos and some China provinces. Due to rapid growth of *Gmelina aborea* majorly for log purposes, this plant is planted expansively in Nigeria, Sierra Leone and Malaysia [57]. The high rate of leaf wastes generated from *Gmelina aborea* litters the ground thus acidifying the soil at some point during its decay processes thereby preventing the invasion of another plant species. Interestingly, *Gmelina aborea* leaf *is* a brittle lignocellulosic material with high carbon content, these properties enhances its processing into powdery form thus making it suitable for adsorption of various contaminants.

Rhodamine B (Rh–B) dyes are water soluble basic red cationic dyes and common water tracer fluorescent owing to their excellent photophysical properties. Rhodamine dyes, which belong to the xanthene class of dyes, are among the oldest synthetic dyes used for the dyeing of fabrics and in food industries. it is established to be harmful when swallowed, with acute oral toxicity, causes serious eye damage or irritation, hazardous to the aquatic environment with long-term effect [58, 59, 60]. Adsorption method using different adsorbents has been used severally for removing RhB dye from aqueous solution [59, 60, 61, 62, 63, 64, 65, 66, 67, 68, 69, 70, 71, 72, 73, 74, 75, 76]. In addition, other method including photocatalytic degradation using MOFs, $SiO_2@TiO_2$ nano-spheres, titania films, titania nanorod thin films, ZnO nanorods, TiO_2 photonic crystals, UV/$S_2O_8^{2-}$, $PbCrO_4/TiO_2$, gelatin/CuS/PVA nanocomposites, MnO_2 nanorods have been used for RhB dye degradations [77, 78, 79, 80, 81, 82, 83, 84, 85, 86, 87, 88, 89].

This study is aimed at preparing, characterizing and applying *Gmelina aborea* leaf (GAL) activated carbon as adsorbent for the removal of RhB dye from aqueous solutions and to study the isotherm, kinetic and thermodynamic parameters governing the adsorption process. The uniqueness of GAL to remove RhB dye from aqueous solution has never been reported in this field, likewise the GAL morphological properties, surface characteristics and pH coupled with its carbonaceous content exemplified by the large surface area, high carbon contents and well-developed pores favors its affinity towards RhB dye adsorption. The influences of operational parameters are also studied for the first time on ability of chemically prepared AC from GAL to adsorb RhB dyes. Comparing with other reported work on RhB dye, this study is majorly focused on the use of functionalized leaf-based adsorbents from *Gmelina aborea* for RhB dye removal from aqueous media. Such study is necessary due to the particularities of these adsorbents in dye adsorption processes, numerous availability at a relative low cost, and numerous activation possibilities. These particularities have been highlighted in this study. Moreover, to the best of our knowledge, this is the first time a study on the utilization of the *Gmelina aborea* leaf adsorbent for RhB dye removal was investigated.

2. Materials and methods

Gmelina aborea leaf (GAL) was collected from LAUTECH Ogbomoso, Nigeria, washed with distilled water and oven dried to constant weight. A carefully weighed 25 g of GAL was then pulverized into tiny particle sizes and was activated chemically using 500 cm^3 of 0.3 mol dm^{-3} of orthophosphoric acid (H_3PO_4) and was stirred. This was afterward heated at a temperature of 300 °C for 60 min in an oven and then allowed to cool. It was then washed with distilled water and later oven dried at a temperature of 105 °C for 4 h to constant weight. The adsorbent was then sieved to 150 μm mesh size and kept in air tight containers for further use.

2.1. Characterization

The characterization of *Gmelina aborea* leaf raw (GALR) and activated samples (GALAC) were carried out using Fourier Transform Infrared (FTIR) FTIR-2000 (Shimadzu Model IRPrestige-21 Spectrophotometer). The spectroscopic analysis was used to study the surface chemistry of GALR and GALAC powder. The FTIR spectra gave detailed characteristics' functional group(s) on the surfaces of both GALR and GALAC. Scanning Electron Micrograph (SEM) was employed to study the surface characteristics and the morphological features of the GALR and GALAC samples. It produces both the quantitative and qualitative information which are further analyzed by a range of detectors to give three-dimensional image(s). Elemental analysis of both GALR and GALAC were carried out using Energy Dispersive X-ray (EDX) to determine the elemental compositions present in the samples before and after acid activation. The resulting elemental analysis line spectrum corresponds to specific elemental composition. The intensities of the characteristics' line are proportional to the elemental compositions which are quantitative in nature.

2.1.1. Determination of oxygen-containing functional groups

This study used Boehm titration method to determine the oxygen containing functional groups [90, 91]. Four portions of 1.0 g each of raw and GALAC samples were kept in contact with separate solutions of 10–15 ml of 0.1 M NaOH, 0.1 M $NaHCO_3$ and 0.05 M Na_2CO_3 for determining acidic groups and 0.1 M HCl for the basic groups composites respectively at temperature of 48 h. Afterwards, the resulting aqueous solutions were back-titrated with 0.1 M HCl for acidic and 0.1 M NaOH

for basic groups. The types and numbers of acidic sites were calculated using previous procedure [45, 53]. Briefly, for the determination of the numbers and types of acidic sites, certain considerations were made that NaOH neutralizes carboxylic, lactonic and phenolic groups, Na_2CO_3 neutralizes carboxylic and lactonic groups and that $NaHCO_3$ neutralizes only carboxylic groups. The amount of oxygen-containing-functional groups, F_x, is calculated using the relation:

$$F_x = \frac{(V_{bx} - V_{ex})}{m_x} \times M_t \times D_F \quad (1)$$

$$D_F = \frac{initial\ volume}{selected\ volume\ for\ titration} \quad (2)$$

where "F_x ($mmolg^{-1}$) is the amount of oxygen containing functional groups, V_{bx} is the volume of titrant used to titrate the blank, V_{ex} is the volume of the titrant used to titrate the extract, M_t is the molarity of the titrant used, D_F is the dilution factor".

2.1.2. pH and point of zero charge (pHpzc) determinations

For the determination of the pH_{pzc} of the GALAC, 0.05 g of GALAC was added into solution containing 100 ml of 0.1M NaCl with known initial pH. NaOH or HCl was used to adjust the pH value. The sample holder was corked and placed in a shaker, agitated for 24 h at 250 rpm, the final pH was then determined. A graph of pH difference, ΔpH (final pH − initial pH) versus the initial pH was used to determine the pH_{pzc}. The pH_{pzc} exists when pH does not change upon a contact with the adsorbent(s).

2.2. Batch equilibrium studies

Batch adsorption method was carried out using UV-Visible spectrophotometer at wavelength of 554 nm. Studies such as the effects of initial dye concentration at five different concentrations: 200, 400, 600, 800 and 1000 mg/L were investigated. Also, the effects of contact time, adsorbent dosage, and solution temperatures (at 303 K, 313 K and 323 K) were studied using standard methods [53, 92]. The adsorbent dosage used throughout the adsorption process was 0.1 g of GALAC. The adsorption process was allowed to proceed in the water bath shaker to equilibrium up to 120 min. Five (5) sets of 100 ml Erlenmeyer flasks containing the mixture of 0.1 g of the sample and the RhB dye solution of different initial dye concentrations were carefully arranged in the shaker, it was then agitated at 120 rpm. The shaker used is a thermostatic water bath shaker filled with water to the level of the arranged flask's solution in order to make the solution temperature uniform to that of the shaker at specified temperature until equilibrium was reached. Sample solutions were withdrawn at a pre-determined time intervals for the determination of residual concentrations using a UV-Vis spectrophotometer. The amount of RhB dye uptake and percentage removal at equilibrium were calculated using Eqs. (3) and (4) respectively:

$$q_e = \frac{(Co - Ce)V}{m} \quad (3)$$

$$\%\ removal = \left[\frac{(Co - Ce)}{Co}\right] x\ 100\% \quad (4)$$

where, C_o and C_e are respective initial and equilibrium dye concentrations ($mg.L^{-1}$), V is the volume of solution (dm^3), m is the mass of adsorbent (g), Q_e is the amount of dye adsorbed ($mg.g^{-1}$).

2.3. Mathematical modeling

2.3.1. Isothermal studies and kinetic models

Four different adsorption isotherm models: Langmuir [93, 94], Freundlich [95], Temkin [96] and Dubinin–Radushkevich (D–R) [97] were employed to test the adsorption data. The detailed isotherm parameters for RhB dye adsorption on *Gmelina aborea* leaf (GALR) are listed in Table 1. Different kinetic models were used to test the adsorption data, they are: pseudo-first-order (PFO) [98], pseudo-second-order (PSO) [99], Elovich [100, 101] and intraparticle diffusion (IPD) [102] models. Table 1 shows the detailed kinetic model parameters for RhB dye adsorption on

Table 1
Adsorption isotherm and kinetics parameters.

Adsorption model	Type	Equation	Expression of the equation	Refs.
Isotherm	Langmuir	$\frac{C_e}{q_e} = \frac{1}{q_m C_e} + \frac{1}{K_L q_m}$ (5) $R_L = \left[\frac{1}{(1 + K_L Co)}\right]$ (6)	C_e is the adsorbate concentration at equilibrium (mg/L), q_e is the amount of adsorbate adsorbed per unit mass of adsorbent ($mg.g^{-1}$), q_m is the maximum monolayer adsorption capacity of the adsorbent ($mg.g^{-1}$), K_L; the Langmuir adsorption constant ($L.mg^{-1}$). C_o is the highest initial solute concentration; whereas, R_L value implies the adsorption is unfavorable {(R_L>1), linear (R_L = 1), favorable (0 <R_L< 1), or irreversible (R_L = 0)}.	[93,94]
	Freundlich	$\ln q_e = \frac{1}{n} ln C_e + ln K_f$ (7)	K_f is the Freundlich isotherm constant (($mg.g^{-1}$) ($L.mg^{-1}$)); n, the heterogeneity factor. The slope of 1/n ranging between 0 and 1 is a measure of adsorption intensity, which becomes more heterogeneous as the values get closer to zero.	[95]
	Temkin	$q_e = B ln K_T + B ln C_e$ (8)	B = R_T/b is the constant related to the heat of adsorption ($L.mg^{-1}$); T is absolute temperature; R is universal gas constant (8.314 J/mol K); K_T, equilibrium binding constant ($L.mg^{-1}$).	[96]
	D–R	$ln q_e = ln q_m + \beta\ \varepsilon^2$ (9) $\varepsilon = RT\left[1 + \frac{1}{C_e}\right]$ (10) $E = \frac{1}{\sqrt{2\beta}}$ (11)	β a constant related to the adsorption energy (mol^2/kJ^2); Ɛ is the Polanyi potential, E is adsorption energy (when value of E is between 1 and 8 kJ/mol, it implies a physical adsorption while value between 9 and 16 kJ/mol means a chemical adsorption.	[97]
Kinetics	PFO	$\ln(q_e - q_t) = ln\ q_e - K_1$ (12)	$q_t$is the amount of solute adsorb per unit weight of adsorbent at time t (mgg^{-1}), K_1 is the pseudo-first order kinetics rate constant (min^{-1}).	[98]
	PSO	$\frac{t}{q_e} = \frac{1}{K_2 q_e} + \frac{1}{q_e}\ t$ (13)	K_2 is pseudo-second order kinetics rate constant (min^{-1}).	[99]
	Elovich	$q_t = \frac{1}{\beta}\ln(\alpha\beta) + \frac{1}{\beta}\ln t$ (14)	α is the initial desorption rate [mg. (g min)$^{-1}$], β, the desorption constant ($g.mg^{-1}$). The 1/b value denotes the number of available sites for adsorption and the value of (1/β); (ln αβ) shows quantity of adsorption when (ln t) equal to zero.	[100, 101]
	IPD	$q_t + K_{diff} t^{1/2} + C$ (15)	C is the intercept and reflects the boundary layer effect of the plot $q_t$against $t^{1/2}$. K_t ($mg/g\ h^{1/2}$) denotes the intra-particle diffusion rate constant; $t^{1/2}$, the half-adsorption time ($h^{1/2}$). For intra-particle diffusion to be the only rate determining step, then the regression of $q_t$against $t^{1/2}$ must be linear and should pass through the origin, otherwise, it then implies that the intra-particle diffusion is not the only rate-controlling step	[102]

Gmelina aborea leaf (GAL).

2.3.2. Thermodynamic studies

Thermodynamic parameters which explain the feasibility, spontaneity and the nature of adsorbate-adsorbent interactions (ΔG°, ΔH° and ΔS°) were calculated from thermodynamic equations (Eqs. (16), (17), and (18)) [53]. These were used to explain the adsorption process at different temperatures (303, 313 and 323 K respectively):

$$\Delta G^{\circ} = -RT \ln K_L \tag{16}$$

$$\ln K_L = \frac{\Delta S^{\circ}}{R} - \frac{\Delta H^{\circ}}{RT} \tag{17}$$

The values of ΔS and ΔH were obtained from the intercept and slope of Van't Hoff plot of $\ln K_L$ against $1/T$. Values of K_L (Langmuir constant in $L.mol^{-1}$) are calculated at 303 K, 313 K, and 323 K respectively. Arrhenius equation was used to calculate the adsorption energy of activation which represents the minimum energy needed by the reactants for the interaction to occur (Eqn 18):

$$\ln K_2 = \ln A - \frac{Ea}{RT} \tag{18}$$

where K_2 is the PSO rate constant (g. $(mg\ h)^{-1}$), E_a is the Arrhenius energy of activation of RhB-dye adsorption, ($kJmol^{-1}$) with A being the Arrhenius factor, R is the gas constant. The plot of $\ln K_2$ versus $1/T$ gives a straight line graph with slope of $-E_a/R$.

3. Results and discussion

3.1. Characterization

3.1.1. Scanning electron microscopy (SEM)

Fig. 1 shows the morphologies of the GALR and GALAC. It can be seen in Fig. 1b that several pores were found on the surface of GALAC with honeycomb shapes as opposed to that found in the raw sample (GALR) with smooth and closed surfaces (Fig. 1a). This indicates that acid activation is more effective in creating well-developed porous surfaces on GALR sample. These pores provide excellent surfaces for trapping and adsorption of RhB dye molecules [4,103,104]. The porosities observed here is a function of pores available for RhB dye uptake which further enhanced the sorption capacity in the GALAC sample. This is due to the breakdown of the lignocellulosic material at high temperature followed by evaporation of volatile compounds present in GALR. The presence of pores and internal surfaces are requisite for effective adsorbent. The simple mechanisms of activation involve decomposition of the tissues of GALRs (which are the carbon precursor) and creation of new pores and voids. H_3PO_4 permeates tiny pores or voids, thereby increasing the contact between the H_3PO_4 in the carbon precursors which further promotes the release of volatile materials from the GAL thus widening the micropores which are finally converted to mesopores.

3.1.2. Energy Dispersive X-Ray

Elemental analysis of both GALR and GALAC were obtained from EDX spectra and data. The spectra of both samples are presented in Fig. 2. The data of EDX analyses for both GALR and GALAC are shown in Table 2. This revealed the amount of carbon and oxygen contents present in the two samples. The GALAC was very high in carbon content and significantly low in oxygen content. The low oxygen contents and high carbon contents are the major requisites for high adsorption capacity. Table 2 revealed that GALAC contained 82.81% by weight and 91.2% by atom of carbon while the GALR contained 74.53% by weight and 85.72 % by atom with oxygen contents higher of than that of GALAC. This implies that GALAC was richer in carbon contents than the GALR owing to the effects of acid activation on GALR sample. Since GALAC is richer in carbon content, it expected that it is an efficient material for dye removal. The lower the oxygen contents the higher the carbon contents of the samples under study, the more efficient the adsorbent. This observation is consistent with studies reported previously [52].

3.1.3. Fourier transform infra –red (FTIR)

The FTIR spectra analysis of both the raw and the activated *Gmelina aborea* leaf are presented in Fig. 3 and Table 3 showing different bands and assigned functional groups. It is evidence from Fig. 3b that the peaks were marginally shifted in comparism with Fig. 3a. These shifts in peak values are attributed to the influence of H_3PO_4 used for modification. The FTIR spectroscopic characteristics are shown in Table 3. The FTIR spectroscopic analysis demonstrated a wide band at 3755.40 cm^{-1}; representing the O–H stretching of alcohol. The bands observed at 3437–3417cm^{-1} showed H-bonded of alcohol. The peaks observed between 2854 and 2922cm^{-1} attributed to the C–H stretching of alkanes. The bands at 2376-2378cm^{-1} representing H–C=O stretch of aldehydes. The peaks at 1913-1867cm^{-1} were assigned to aromatic –C≡ C-stretch of alkynes and those observed at1720- 1705cm^{-1} indicating a C=O stretch of lactones, ketones and carboxylic anhydrides. The bands around 1641-1633cm^{-1} show the presence of N=H bonds of primary amines. N–H asymmetric stretch was observed at 1529- 1512cm^{-1}. The band around 1458-1442cm^{-1} shows that C–H bending of alkanes is present in the sample. The bands observed at 1386-1384cm^{-1} represents C–H bending of alkanes. The peak shown at 1259cm^{-1} represents O–H wag (-CH_2X) of

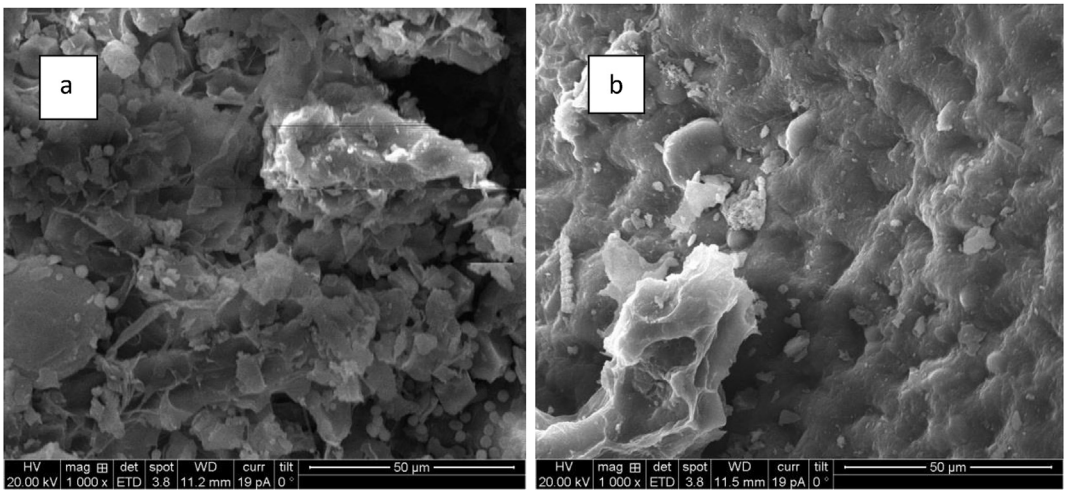

Fig. 1. SEM image of (a) Raw *Gmelina aborea* Leaf (b) Activated *Gmelina aborea* Leaf.

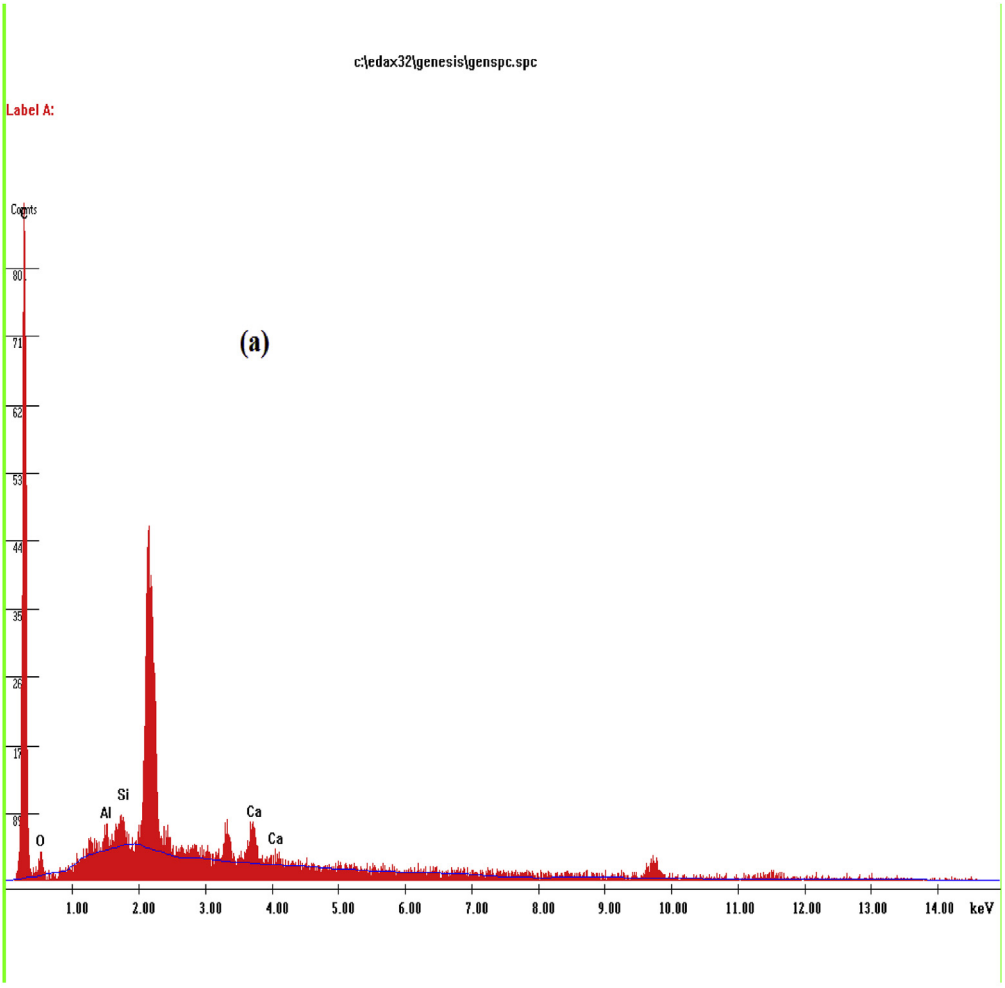

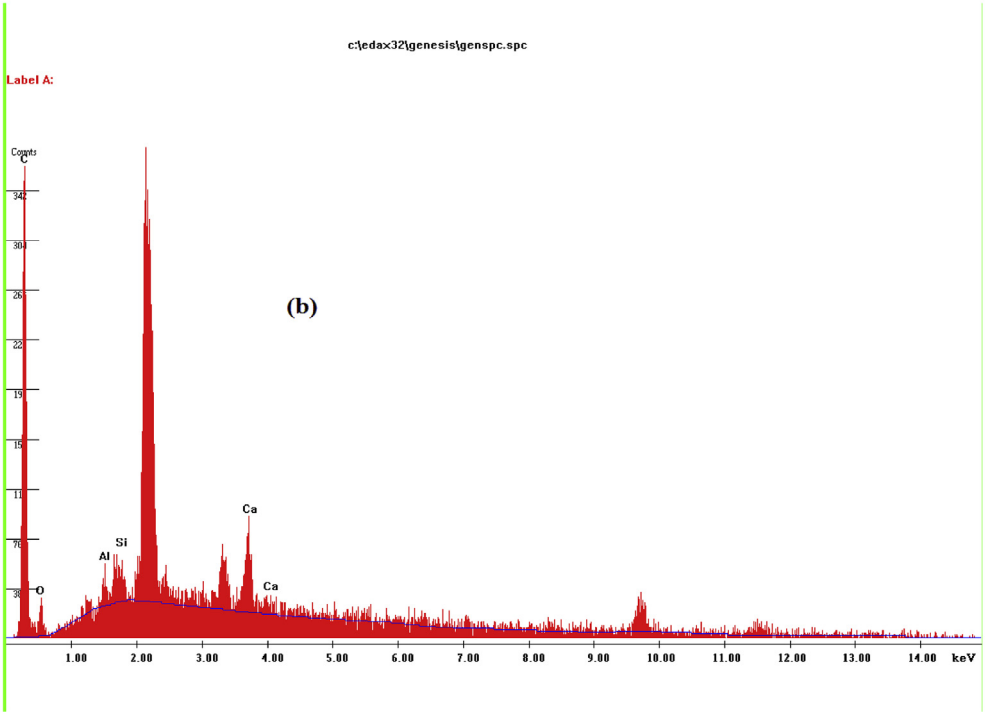

Fig. 2. EDX spectrum of (a) GALR (b) GALAC.

Table 2
EDX results of GALR and GALAC.

Element	Wt%	At%	K-Ratio	Z	A	F
GALR						
C	74.53	85.72	0.4569	1.0154	0.6037	1.0001
O	9.18	7.93	0.0164	0.9963	0.1795	1.0001
Al	2.14	1.1	0.0171	0.9209	0.863	1.0022
Si	2.52	1.24	0.0217	0.9409	0.9147	1.0021
Ca	11.62	4.01	0.1081	0.9146	1.0167	1
Total	100	100				
GALAC						
C	82.81	91.2	0.327	1.013	0.3897	1
O	3.95	3.27	0.0074	0.994	0.1881	1.0001
P	11.94	5.1	0.1077	0.906	0.9952	1.0005
Ca	1.29	0.43	0.0119	0.9121	1.0058	1
Total	100	100				

alkyl halides. The band observed between 1159-1176cm^{-1} represents C–N stretch of aromatic amine and C–N stretch of aliphatic amine was observed at 1066cm^{-1}. The corresponding band at 665–696 cm^{-1} was assigned to C≡C bending alkynes. The peak observed between 437-441cm^{-1} shows C–Br stretch of alkyl halides. As shown in Table 3, spectra analysis before and after activation. *Gmelina aborea* leaf demonstrated that mostly O–H groups, C–N stretch, C–Br stretch and C–H stretching were engaged during the activation step. Reduction and broadening of bands validate the effectiveness of the activation process. The changes seen in GALAC FTIR spectra confirmed the effects of H_3PO_4 activation of GALR giving good indications of the suitability of the GALAC for effective RhB dye removal from aqueous solutions. Similar observations have been reported previously [52].

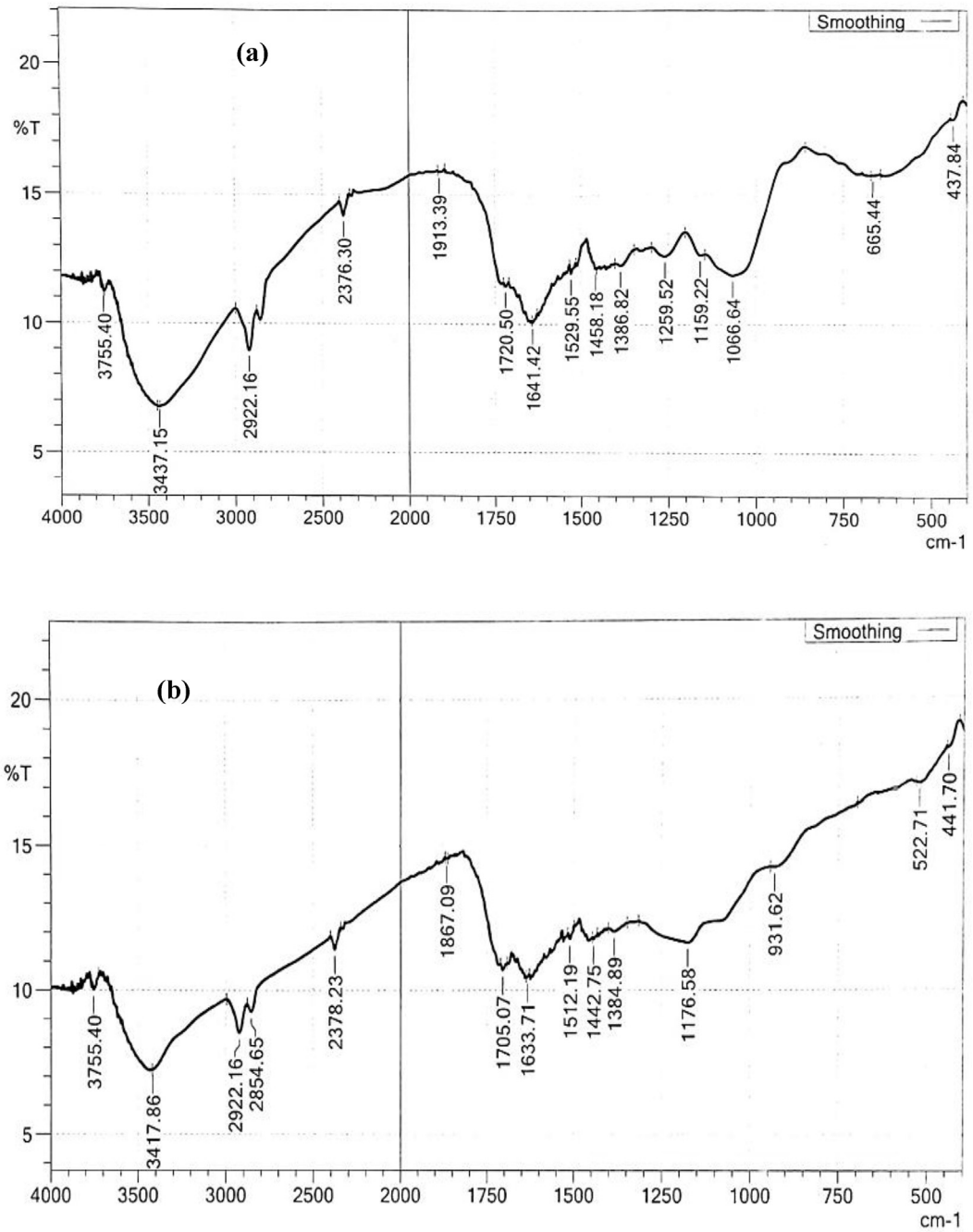

Fig. 3. (a) FTIR spectra of the raw *gmelina aborea* leaf (GALR). (b) FTIR spectra of acid activated *gmelina aborea* leaf (GALAC).

Table 3
Functional group presents in GALR and GALAC.

Wavenumber (cm^{-1})			Band
GALR	GALAC	Differences	
3755	3755	0	O–H stretch of alcohol
3437	3417	-19	O–H stretch of alcohol
2922	2922	0	C–H stretch of alkanes
—	2854	0	C–H stretch of alkenes
2376	2378	2	H–C=O stretch of aldehydes
1913	1867	-46	-C≡C- stretch of alkynes
1720	1705	-15	C=O stretch of β- unsaturated
1641	1633	-8	-C=C-stretch of alkenes
1529	1512	-17	C–C stretch of aromatics
1458	1442	-15	C–H bend of alkanes
1386	1384	-2	C–H bend of alkanes
1259	—	—	C–H wag of alkyl halides
1066	—	—	C–N stretch of aliphatic amines
665	—	—	C–Br stretch of alkyl halides
437	441	4	C–Br stretch of alkyl halides

3.1.4. *Boehm Titration and pH_{pzc}*

The surface functional groups and pH_{pzc} are significant parameters governing RhB dye adsorption onto GALAC. These parameters are used to explain the adsorbents' acidities and/or basicity, types of AC (H- or L-type) and also the carbon's net surface charge in solution. It must be noted that AC contained both acidic and basic groups. The acidic functional groups include phenolic, lactonic and carboxylic [105] while the basic groups are the oxygen-containing species including pyronic, ketonic, chromenic, and p-electron system(s) of carbon basal plane(s) [106]. The nature and preparation condition of AC determines the density of surface functional groups of the precursors. In this study, H_3PO_4 greatly increased the density of GAL surface functional groups thereby improving the functional group interactions with polar solute from the solutions. The Boehm technique reveals the surface chemical properties of the adsorbents. Table 4 presents a summary of the properties of the surface functional groups. To evaluate the surface acidity and basicity of GAL; two assumptions were made: (i) acidic groups would only be neutralized by NaOH, Na_2CO_3 or $NaHCO_3$ and (ii) all basic groups are neutralized by HCl. The concentration of the acidic and basic groups are shown in Table 4, The basic group value was lower than the acidic group indicating that the adsorbent surface is predominantly acidic, Similar result was obtained in the adsorption of Ba^{2+} and Fe^{2+} ions [107] from aqueous solutions using activated carbon produced from mazot ash [108]. Acidic functional groups results in increased adsorption of RhB dye molecules [109,110].

The pH_{pzc} (which is the pH where the net carbon surface charge equals zero) was determined by the combined influences of all the AC functional groups. The GALAC surface charge was determined by pH of the RhB dye solution. It has been established that a net positive charge on carbon surface are obtained when the pH of the solution is lower than the pH_{pzc} and a negative charge predominates when the pH of the solution is higher than pH_{pzc}. To determine pH_{pzc}, ΔpH was plotted against pH_o as shown in Fig. 4. The final pH_f plateau was obtained in Fig. 4 corresponding to a pH where no net H^+ or OH^- adsorptions, implying that at this point, the difference between final [H^+] and initial [OH^-] is zero. The pH_{pzc} (Fig. 4) was observed to be 5.75 for GALAC. Cationic adsorption is favored when pH_{pzc} is lesser than pH while adsorption of anions are enhanced at pH less than pH_{pzc} [111, 112]. The total acidic groups determined by Boehm titration for the GALAC is 0.125 mmol/g while the basic group was 0.094 mmol/g (Table 2), this suggests that the adsorbent surface was predominantly acidic. Therefore, the acidic groups resulted in greater number of oxygenated-functional groups on the surface of the GALAC [109]. Therefore, RhB dye–adsorption increased at pH higher than the pH_{pzc}.

Table 4
Different functional groups on GALAC.

Adsorbent	Carboxylic groups (mmol/g)	Lactones (mmol/g)	Basicity (mmol/g)	Acidity (mmol/g)
GALAC	0.2000	0.075	0.094	0.12500

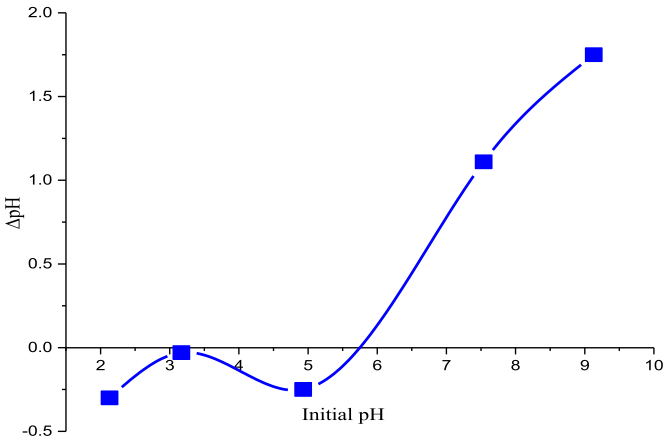

Fig. 4. Plot of point zero charge of acid Activated *Gmelina aborea* Leaf (GALAC).

3.2. *Operational parameters*

3.2.1. *Initial RhB dye concentration and contact time*

The RhB dye uptake by GALAC as a function of different initial Rh.B dye concentrations (200–1000 mg/L) and temperatures of 303, 313, and 323K were investigated. The RhB dye uptake at 303K is shown in Fig. 5. The amount of RhB dye adsorbed increased with increased initial RhB dye concentrations. The increase in initial dye concentrations gave the driving force required to break the mass transport barriers that resist the interactions of RhB dye between the solid and aqueous phases. Thus, the comparative patterns were observed at higher temperatures. The RhB dye uptake (q_t) was very rapid at the initial stages of the contact period around 0–15 min but after 15 min it became very slow, it reaches equilibrium before 40 min. This was attributable to the availability of larger numbers of vacant sites accessible for Rh.B dye adsorption during the initial stages [10]. After a lapse of time, the adsorption became slower as a result of the decreasing number of vacant sites since these surface sites were almost fully occupied by dye molecules. The progressive slow adsorption toward equilibrium was most likely due to the saturations of active sites. It can be inferred here that the contact time required for Rh.B

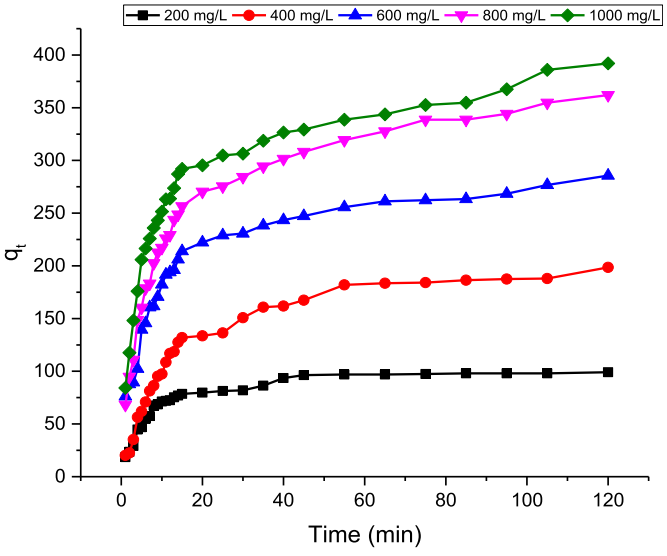

Fig. 5. Plot of Rh–B dye adsorption uptake against adsorption time at 323 K.

dye with initial concentrations of 200–600 mg/L to achieve equilibrium was 35 min. Conversely, for 800–1000 mg/L initial concentrations, the equilibrium was reached between 95-105 min. This is so because, the Rh.B dye molecule(s) needs to firstly encounter the boundary layer effects first prior to a diffusion onto the adsorbent's surfaces, thereafter, it diffuses into the adsorbent's porous structures [113]. In fact, at higher initial dye concentrations, the higher Rh.B dye uptake was obtained as the numbers of dye molecules contending for the sites available on the GALAC surface are higher. This means that Rh.B dye solutions having higher concentration (for this study; 800–1000 mg/L) would require longer time period to reach equilibrium. The adsorption uptakes of Rh.B dye at equilibrium shows that the process of adsorption is majorly initial Rh.B dye concentrations dependent [39, 53, 113].

3.2.2. Effect of solution temperature

The Fig. 6 reveals the extent of adsorption of Rh.B dye against the solution temperature for the GALAC at 323 K. The amount of RhB dye adsorbed (q_m (mg/g)) increase from 142.86 mg/g to 1000 mg/g as the solution temperature increases from 303 K to 323 K. This means that; increasing the temperature resulted into rapid mobility of RhB dye to interact with the GALAC active sites and also facilitate the adsorbent pores, both on the internal boundary layers and on the surface (external boundary layers) as the solution viscosity decreased at high temperature. This thereby created a networked linkage between the pores which significantly enhanced the GALAC to trap more RhB dye molecules thereby enhancing the affinity of GALAC surface to trap RhB dye molecules. This observation indicates an endothermic process of adsorption. Adsorption process was favored by increase in temperature of the interaction. This was due to large available surface areas and aggregate pore volumes of GALAC. Therefore, since reactions at 323 K shown a prevalence and significant adsorption yields, it was selected as the optimum temperature for RhB dye adsorption onto GALAC. Similar pattern have been observed in other studies [29].

3.2.3. Effect of pH on adsorption of RhB dye

pH of the solution has a profound influence on adsorption process; it determines both the extent of adsorption of the dye molecule and the surface charge of the adsorbent. The effect of pH on the uptake of RhB dye onto GALAC was investigated and the highest percentage of RhB dye adsorbed was obtained at pH 3 (91 %) (Fig. 4). A gradual decrease was observed at pH above 3. The lowest amount of RhB dye adsorbed was at pH 10 (30 %). RhB dye has a pK_a value of 3.7. At this pK_a, it exists as cationic, lactonic or zwitterionic forms depending on the solution media. At pH value lower than pH_{pzc} (5.75), the RhB dye are of cationic and

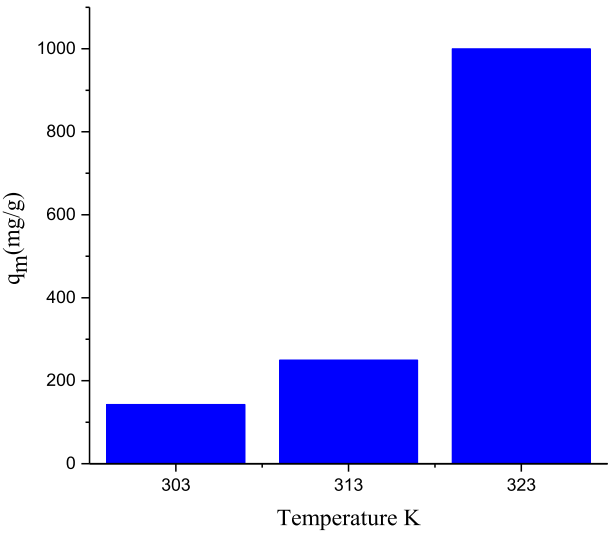

Fig. 6. Effect of temperature on the adsorption of RhB dye onto GALAC.

monomeric molecular forms [114], thus the dye molecule can enter easily into the pore structure of GALAC. At pH value higher than pH_{pzc}, the zwitterionic forms of RhB dye exist in solution mixture. This form increases the aggregation of RhB dye molecule to form larger molecules (dimers). The increase in aggregation of the zwitterionic form is due to the attractive electrostatic interactions between the carboxyl and xanthene groups of the monomers [115]. These molecules are unable to enter the pores as a result of their size thereby resulting in lower percentage removal at high pH. Optimum adsorption at pH of 3 has been previously reported in one of our studies [53, 108].

3.3. Adsorption equilibrium and isotherms

Figs. 7(a-d) shows the plot of Langmuir, Freundlich, Temkin and D-R isotherms for the RhB dye uptake onto GALAC. Their corresponding isotherm parameters were determined from slope and intercept of each plot. The adsorption parameters obtained from Langmuir, Freundlich, Temkin and DBR isotherm plots are presented in Table 5. The best equilibrium was obtained on the basis of linear regression correlations (R^2). Contrast to other isotherms, Langmiur model has the highest regression values ($R^2 = 0.9941$, $R^2 = 0.9930$, $R^2 = 0.9999$) at 303 K, 313 K, and 323 K respectively. Temperature of 323 K gave the best fit judging from the R^2 values. In the present study, Langmuir equation was also expressed in term of dimensionless separator factor (R_L). Increase in Langmuir isotherm separation factor (R_L) from 0.482 to 0.5 (Table 5) with increase in temperature indicates that the adsorption is favorable at higher concentration leading to a gradual decrease of K_L. This suggests that the process of adsorption was favored at higher initial Rh.B dye concentrations. The value of q_m value (q_m = 1000 mg/g) obtained for RhB dye adsorption onto GALAC was compared with other sorbents [47, 49, 50, 51, 53, 55, 58, 116, 117, 118, 119, 120, 121, 122] (Table 6), GALAC exhibited higher performance. These results show that acid modification largely enhance the adsorption capacity from 142.86 to 1000 mg L^{-1} (Table 5) implying that H_3PO_4 modification resulted in the creation of several pores on GALAC thereby improving the adsorption capacity. The K_F values obtained from Freundlich isotherm demonstrate that a physical process was reasonably part of the sorption process. The higher the value of K_F, the higher the adsorption capacity. The "n" values were used to measure the linear deviation of the adsorption and the adsorption types. In this study, the "n" values were greater than 1 suggesting a favorable adsorption process [123]. The Temkin isotherm parameters are listed in Table 5; the R^2 for GALAC is 0.9918 at 323 K indicating that Temkin parameters account for GALAC-RhB dye interactions. The Temkin isotherm constants (B_T) were positive at all temperatures, this suggests that the system was an endothermic process. The values of E_a obtained from DBR isotherm were found to be 79.52, 22.36 and 74.54 at 303K, 313K, and 323K respectively confirming that the adsorption processes follows physio-sorption mechanisms. Comparing the correlation (R^2) values for the four isotherms, parameters, one can easily conclude that Langmuir isotherm described the adsorption process most. The sequence is Langmuir ($R^2 = 0.9999$) > Temkin ($R^2 = 0.9918$) > Freundlich ($R^2 = 0.9752$) > DBR ($R^2 = 0.9182$) respectively.

3.4. Adsorption kinetics and mechanistic studies

The kinetics of adsorbate uptake is essential for selecting optimum operating conditions for the process design. These adsorption data were analyzed using PFO (Fig. 8a) [98], PSO (Fig. 8b) [99], Elovich (Fig. 8c) [100,101] and IPD (Fig. 8d) [102] models. As presented in Fig. 8b, and Table 7, the pseudo-second-order (PSO) kinetics best described the adsorption kinetic process of RhB dye onto GALAC. Elovich model was used to depict the second-order kinetics by assuming that the actual solid surfaces are energetically heterogeneous. Comparing the R^2 values obtained in the adsorption process, the suitability of the kinetic isotherms fit for the adsorption data follows the order: PSO > PFO > Elovich. The mechanism of adsorption was investigated using intraparticle diffusion

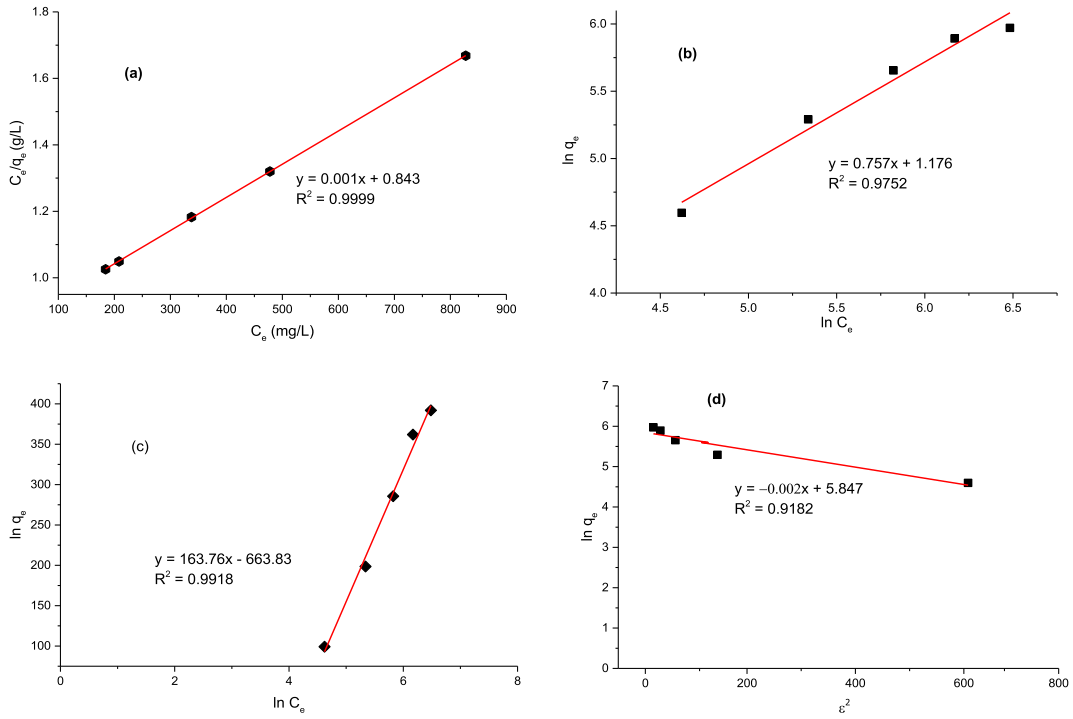

Fig. 7. (a)Plot of Langmuir isotherms for Rh–B dye adsorption onto GALAC. (b) Plot of Freundlich isotherm for Rh–B dye adsorption onto GALAC. (c) Plot of Temkin isotherm for Rh–B dye adsorption onto GALAC. (d) Plot of Dubinin-Radushkevich isotherm for Rh–B dye adsorption onto GALAC.

Table 5
Different isotherm parameters for the adsorption of Rh.B dye unto GALAC.

Isotherms	Tempratures		
	303 K	313 K	323 K
Langmiur			
q_m (mg/g)	142.86	250	1000
K_L	0.0172	0.006	0.0003
R_L	0.482	0.499	0.5
R^2	0.9941	0.9930	0.9999
Freundlich			
n	41.67	2.398	5.952
K_f	95.78	12.77	64.07
R^2	0.987	0.959	0.9752
Temkin			
A	0.091	2.852	2.195
B_t	106.2	56.4	0.946
R^2	0.9650	0.9551	0.9981
DBR			
B	-7.00E-05	-1.00E-03	-9.00E-05
q_o	110.72	195.97	156.35
E_a	79.515	22.361	74.536
R^2	0.9942	0.9910	0.9182

Table 6
Comparison of adsorption capacities of different dyes onto various adsorbents.

Adsorbents	Dye	q_{max} (mg/g)	Refs
NaOH-modified durian leaf	Methylene Blue	125	[50]
NaOH-modified dead leaves of plane trees	Methylene Blue	145.62	[51]
Surfactant ($C_{19}H_{42}BrN$)-modified *Prunus Dulcis* leaves	Acid blue 113	97.09	[49]
NaOH-modified *Ficusracemosa* with	Acid blue 25	83.33	[47]
Citric acid-modified *ricinuscommunis* leaves	Methylene Blue	81.29	[116]
H_3PO_4-modified berry leaves with	Eriochrome Black T	133.33	[55]
Surfactant (HDTMA-Br)-modified pineappleleaf	Methylene blue	52.6	[117]
Surfactant (HDTMA-Br)-modified pineappleleaf	Methyl orange	47.6	[117]
HCl-modified Calotropis procera leaf	Methylene Blue	192.31	[118]
Sulfonic acid-modified tea leaf	RhodamineB	757.6	[119]
Bagasse pith	Rhodamine B	263.85	[120]
Aleurites moluccana seeds	Rhodamine B	117	[121]
Rice husk-based	Rhodamine B	478.5	[122]
KOH-treated Irvingia gabonensis	Rhodamine B	232	[58]
Moringa oleifera seed pod	Rhodamine B	1250	[53]
H_3PO_4-modified *Gmelina aborea*	Rhodamine B	1000	*This study*

(IPD) model. As indicated by IPD model, the values of q_t were observed to vary linearly with the value of $t^{1/2}$. The rate constant, k_{diff} presented in Table 7 was determined from the slope of the graph (Fig. 8d). The plots obtained were non-linear. The first adsorption phase is bulk diffusion while the second phase is intraparticle mass transfer resistance. The rate at which the equilibrium is attained is IPD-controlled [124]. The RhB dye uptake onto GALAC at different initial dye concentration (Fig. 8d) gave multilinear profiles which imply that the sorption process occurred in two stages. The first stage is the boundary layer diffusion of the RhB dye molecules onto GALAC, which is a steeper portion while the second stage is linear and gradual adsorption stage revealing that IPD was the rate determining step. However, it was observed that K_{t2} parts were characterized by the IPD established to be the rate determining step. The plots with non-zero origin ($C \neq 0$) showed an occurrence of IPD in the adsorption process. The deviations from the origin show that IPD was not the only rate-controlling step. The intercept "C" showing a proportionality relationship with boundary layers having the observable extent of thickness at the highest temperature under study 323 K [53,125]. It was observed that the second adsorption stage is considered as the IPD that controls the rate of adsorption process.

3.5. Thermodynamic studies

Thermodynamic parameters such as ΔG, ΔH and ΔS are significant features in adsorption systems [108]. The values of ΔG, ΔH and ΔS were

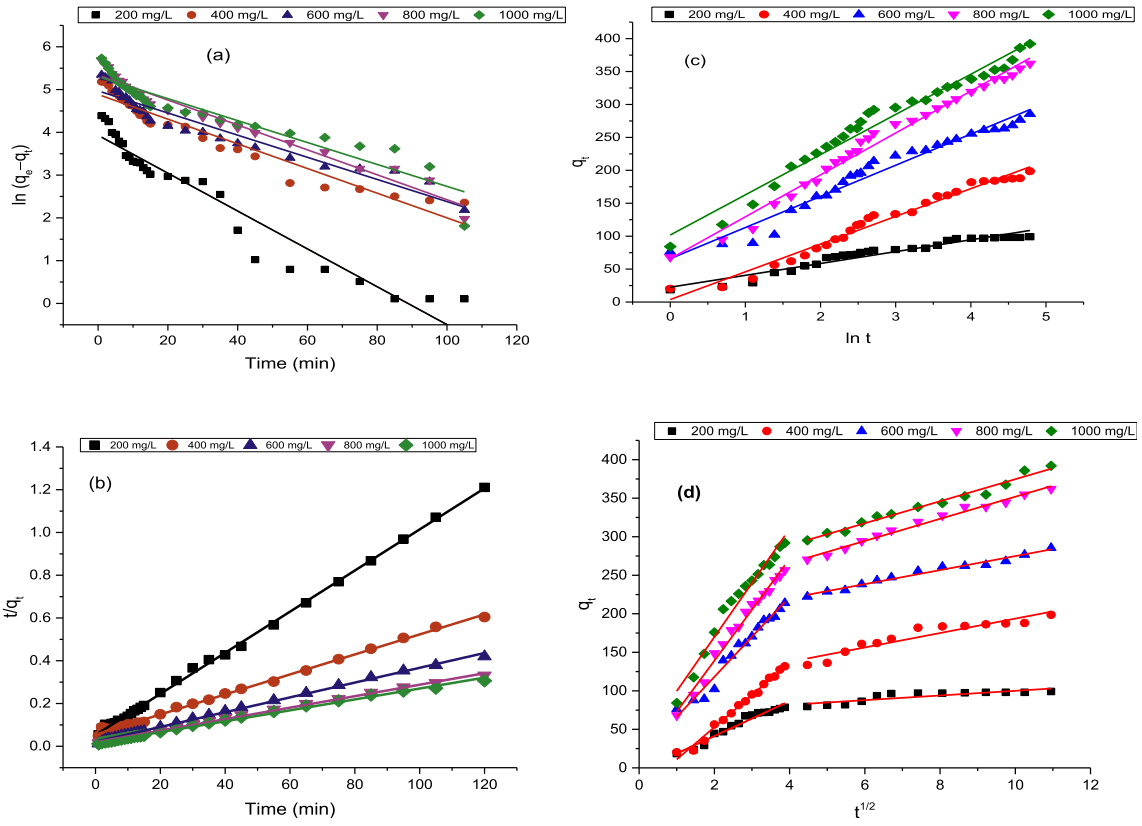

Fig. 8. Plots of (a) Pseudo-first order kinetic, Pseudo-second order kinetic, (c) Elovich and (d) Intraparticle diffusion for Rh–B dye adsorption onto GALAC at 323K.

Table 7
Adsorption Kinetics studies parameters for the adsorption of Rh–B dye on acid activated GALR at 323K.

Kinetics	Initial Rh–B concentrations				
	200 mg/l	400 mg/l	600 mg/l	800 mg/l	1000 mg/l
PFO					
q_{eexp} (mg/l)	126.87	155.08	187.59	154.2	186.44
q_{ecal} (mg/l)	61.93	63.31	100.08	74.59	72.39
k_1 (min)	0.019	0.026	0.022	0.021	0.018
SSE%	12.494	17.99	16.84	15.32	21.94
R^2	0.926	0.97	0.926	0.989	0.99
PSO					
q_{eexp} (mg/l)	126.87	155.08	187.59	154.2	186.44
$q_{eca\ l}$ (mg/l)	125	166.67	200	166.7	200.2
k_2 (min)	1.33E-03	1.33E-03	6.76E-04	1.03E-03	1.09E-03
H (mg/gmin)	20.78	27.03	28.52	37.02	43.48
SSE (%)	0.352	3.954	13.821	12.467	22.57
R^2	0.994	0.997	0.993	0.99	0.994
Elovich					
Bl0.058	0.049	0.037	0.05	0.056	
A.0.773	0.221	0.304	0.804	1.72	
R^2	0.973	0.94	0.971	0.916	0.953
IPD					
K_{diff}	15.65	23.02	21.99	4.896	13.7
C	28.22	37.12	42.17	89.77	85.33
R^2	0.945	0.931	0.945	0.827	0.946
K_{diff}	4.92	4.78	9.42	24.14	6.04
C	68.74	103.8	85.77	22.23	115.4
R^2	0.923	0.957	0.93	0.913	0.934

calculated using Eqs. (16), (17), and (18). The values of ΔS° and ΔH° are obtained from the intercept and slope of Van"t Hoff plot of 1/T against In K_L as shown in Fig. 9 which agreed well with our previous studies on malachite green dye adsorption onto rambutan seed activated carbon [4]. The thermodynamic parameters (Table 8) indicate that the value ΔH was 11.51 kJ/mol; this positive value reveals an endothermic nature of the process of adsorption. The positive value of (ΔS, 0.388 kJ/mol K) revealed that the affinity of adsorbent for RhB dye uptake occurred with increasing randomness at the interface of GALAC-RhB dye system [108, 126]. However, ΔG values were -22.71, -19.56, and -18.19 kJ/mol at 303K, 313K, 323K respectively, confirming that the process of adsorption was endothermic, with an increase in degree of disorderliness. This also depicts the feasibility and spontaneity of the process of adsorption having higher preference for the RhB dye uptake onto GALAC surface. This demonstrates the affinity of GALAC towards the RhB dye [2,38]. Likewise, the energy value (E_a) (i.e. minimum energy E_a needed for reaction to occur) obtained is in the range of 1–80 kJ/mol. Since the value of E_a obtained were less 80 kJ/mol, it suggests that the process of adsorption followed physio-sorption mechanism. These observations agreed with other findings reported in several studies [4, 39, 76, 108, 127, 128].

3.6. Regeneration and recycling studies

Three different solvents were used for regeneration studies: HCl, NaOH and H_2O respectively. The effect of various solvents used for desorption studies indicated that HCl was the best reagent for regeneration studies because 50 mg/l, 40 mg/l and 30 mg/l of adsorbed RhB dye molecules were obtained after 15 h of contact between the loaded matrix and the regenerating agents, It was also observed that equilibrium was reached in 12 h (Fig. 8). Under acidic conditions, RhB dye is displaced by protons from their binding sites. This is expected because regeneration depends on size of the molecule, number of contact points, surface concentration, temperature and concentration of adsorbed species in solution [129]. The regenerated adsorbent was subjected to recycling studies through regeneration step in between. The regeneration efficiency increased from 80.26 to 92.74% when 0.5 M HCl was used in desorbing RhB dye from GALAC. There was a decrease in efficiency when the

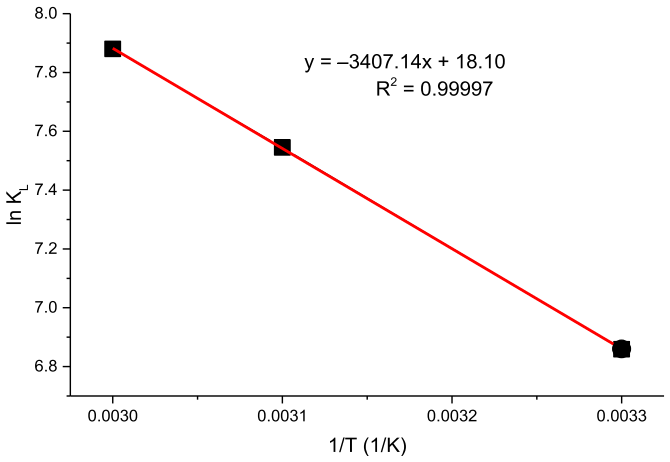

Fig. 9. Van't Hoff plot of 1/T against In K_L for Rh–B dye adsorption onto GALAC.

Table 8
Thermodynamic parameters for the adsorption of Rh.B dye unto GALAC at different temperatures.

ΔH (kJmol^{-1})	ΔS (kJmol^{-1}K)	E_a (kJmol^{-1})	ΔG (kJmol^{-1})		
			303 K	313 K	323 K
11.51	0.39	5.67	-22.71	-19.56	-18.19

Table 9
Price difference between GALAC and CAC.

Cost Description	Price (USD)	
	GALAC (1 kg)	CAC (1 kg)
Cost of purchase	-	376.45
De-ionized water	7.76	-
Electricity	3.22	-
o-phosphoric acid	14.89	-
Transportation	8. 02	11.3
Filter paper	2.45	-
Total	36.34	387.75
Difference (CAC- GALAC)	351.41	

adsorbent was used without HCl treatment (Table 9).

3.7. Cost analysis

The cost analysis presented in Table 9 provides a simple proof that GALAC is approximately eleven times cheaper than CAC providing a saving of 351.41 USD/kg. CAC costs 387.75 US$ per kg (transportation inclusive) in total, while GALAC preparation and transportation costs 36.34 US$ per kg. The low cost of preparing GALAC as stated in Table 9 gave detailed summary of prices from GAL transportation to filtration and washing of the AC. Ortho-phosphoric acid, deionized water and transportation are the major significant costs (Table 9).

4. Conclusion

The study showed that GALAC absorbent could be effectively used in the removal of RhB dye from aqueous solution. The GALR and GALAC adsorbents were characterized using SEM, FTIR, EDX, pH_{pzc} and Boehm Titration (BT techniques respectively. The adsorption of RhB dye on GAL was best described by Langmuir Isotherm model with maximum monolayer coverage of 1000 mg g^{-1}. Adsorption kinetics data was best described by pseudo-second-order kinetics model. Thermodynamic parameters obtained for GALAC (ΔG^o ranges from -22.71 to -18.19 kJmol^{-1}; ΔH^o 1.51 kJmol^{-1}; and ΔS^o 0.39 kJmol-1 K^{-1}) indicates that the removal of RhB dye from aqueous solution by GAL was spontaneous, thermodynamically feasible and endothermic in nature. The cost analysis established that GALAC is approximately eleven times cheaper than CAC. Acid treated *Gmelina aborea* leaf (GALAC) was found to be an effective absorbent for the removal of RhB dye from aqueous solutions.

Declarations

Author contribution statement

Olugbenga Solomon Bello: Conceived and designed the experiments; Analyzed and interpreted the data; Contributed reagents, materials, analysis tools or data; Wrote the paper.

Esther Oluwadamilola Alabi, Kayode Adesina Adegoke, Samuel Adewale Adegboyega, Adejumoke Abosede Inyinbor, Adewumi Oluwasogo Dada: Performed the experiments; Analyzed and interpreted the data.

Funding statement

This work was supported by The World Academy of Science (TWAS) in form of Research grants; Research Grant number: 11–249 RG/CHE/AF/AC_1_UNESCO FR: 3240262674 (2012), 15–181 RG/CHE/AF/AC_1_:3240287083 (2015) for the purchase of Research Equipments, NRF-TWAS Doctoral scholarship award given to the third author (UID: 105453 & Reference: SFH160618172220) respectively and LAUTECH 2016 TET Fund Institution Based Research Intervention (TETFUND/DESS/UNI/OGBOMOSO/RP/VOL. IX) given to the corresponding author respectively.

Competing interest statement

The authors declare no conflict of interest.

Additional information

No additional information is available for this paper.

References

[1] K.A. Adegoke, R.O. Oyewole, B.M. Lasisi, O.S. Bello, Abatement of organic pollutants using fly ash based adsorbents, Water Sci. Technol. 76 (2017) 2580–2592.
[2] M.A.A. Ahmad, O.S. Bello, M.A.A. Ahmad, Adsorption studies of Remazol brilliant blue R dye on activated carbon prepared from Corncob, Am. J. Mod. Chem. Eng. 1 (2014) 1–12.
[3] K.A. Adegoke, O.S. Bello, Dye sequestration using agricultural wastes as adsorbents, Water Resour. Ind. 12 (2015) 8–24.
[4] M.A. Ahmad, N.S. Afandi, K.A. Adegoke, O.S. Bello, Optimization and batch studies on adsorption of malachite green dye using rambutan seed activated carbon, Desalin. Water Treat. 57 (2016) 21487–21511.
[5] A.A. Adeyemo, I.O. Adeoye, O.S. Bello, Adsorption of dyes using different types of clay: a review, Appl. Water Sci. 7 (2017) 543–568.
[6] O.S. Bello, K.A. Adegoke, A.A. Olaniyan, H. Abdulazeez, Dye adsorption using biomass wastes and natural adsorbents: overview and future prospects, Desalin. Water Treat. 53 (2015) 1292–1315.
[7] I.A.W. Tan, B.H. Hameed, Adsorption isotherms, kinetics, thermodynamics and desorption studies of basic dye on activated carbon derived from oil palm empty fruit bunch, J. Appl. Sci. 10 (2010) 2565–2571.
[8] F. Ahmad, W.M.A.W. Daud, M.A. Ahmad, R. Radzi, Using cocoa (Theobroma cacao) shell-based activated carbon to remove 4-nitrophenol from aqueous solution: kinetics and equilibrium studies, Chem. Eng. J. 178 (2011) 461–467.
[9] K. Mahmoudi, K. Hosni, N. Hamdi, E. Srasra, Kinetics and equilibrium studies on removal of methylene blue and methyl orange by adsorption onto activated carbon prepared from date pits-A comparative study, Korean J. Chem. Eng. 32 (2014) 274–283.
[10] I.A.W. Tan, A.L. Ahmad, B.H. Hameed, Adsorption of basic dye on high-surface-area activated carbon prepared from coconut husk: equilibrium, kinetic and thermodynamic studies, J. Hazard. Mater. 154 (2008) 337–346.

[11] O.S. Bello, K.A. Adegoke, A.A. Olaniyan, H. Abdulazeez, Dye adsorption using biomass wastes and natural adsorbents: overview and future prospects, Desalin. Water Treat. 53 (2015) 1292–1315.

[12] Y. Xue, H. Hou, S. Zhu, Adsorption removal of reactive dyes from aqueous solution by modified basic oxygen furnace slag: isotherm and kinetic study, Chem. Eng. J. 147 (2009) 272–279.

[13] S. Nethaji, A. Sivasamy, A.B. Mandal, Adsorption isotherms, kinetics and mechanism for the adsorption of cationic and anionic dyes onto carbonaceous particles prepared from Juglans regia shell biomass, Int. J. Environ. Sci. Technol. 10 (2013) 231–242.

[14] M.A. Islam, M.J. Ahmed, W.A. Khanday, M. Asif, B.H. Hameed, Mesoporous activated coconut shell-derived hydrochar prepared via hydrothermal carbonization-NaOH activation for methylene blue adsorption, J. Environ. Manag. 203 (2017) 237–244.

[15] O.S. Bello, M. Auta, O.B. Ayodele, Ackee apple (Blighia sapida) seeds: a novel adsorbent for the removal of Congo Red dye from aqueous solutions, Chem. Ecol. 29 (2013) 58–71.

[16] S. Gupta, B.V. Babu, Modeling, simulation, and experimental validation for continuous Cr(VI) removal from aqueous solutions using sawdust as an adsorbent, Bioresour. Technol. 100 (2009) 5633–5640.

[17] O.S. Bello, Adsorptive removal of malachite green with activated carbon prepared from oil palm fruit fibre by KOH activation and CO 2 Gasification, South Africa, J. Chem. 66 (2013) 32–41.

[18] A. Bhatnagar, A.K. Jain, A comparative adsorption study with different industrial wastes as adsorbents for the removal of cationic dyes from water, J. Colloid Interface Sci. 281 (2005) 49–55.

[19] M. Visa, C. Bogatu, A. Duta, Simultaneous adsorption of dyes and heavy metals from multicomponent solutions using fly ash, Appl. Surf. Sci. 256 (2010) 5486–5491.

[20] M. Visa, L. Andronic, D. Lucaci, A. Duta, Concurrent dyes adsorption and photo-degradation on fly ash based substrates, Adsorption 17 (2011) 101–108.

[21] A. Mittal, J. Mittal, A. Malviya, D. Kaur, V.K. Gupta, Decoloration treatment of a hazardous triarylmethane dye, Light Green SF (Yellowish) by waste material adsorbents, J. Colloid Interface Sci. 342 (2010) 518–527.

[22] N. Gupta, A.K. Kushwaha, M.C. Chattopadhyaya, Adsorption studies of cationic dyes onto Ashoka (Saraca asoca) leaf powder, J. Taiwan Inst. Chem. Eng. 43 (2012) 604–613.

[23] Y. Wang, L. Zhao, J. Hou, H. Peng, J. Wu, Z. Liu, X. Guo, Kinetic, isotherm, and thermodynamic studies of the adsorption of dyes from aqueous solution by cellulose-based adsorbents, Water Sci. Technol. 77 (2018) 2699–2708.

[24] A. Demirbas, Agricultural based activated carbons for the removal of dyes from aqueous solutions: a review, J. Hazard. Mater. 167 (2009) 1–9.

[25] M.T. Yagub, T.K. Sen, S. Afroze, H.M. Ang, Dye and its removal from aqueous solution by adsorption: a review, Adv. Colloid Interface Sci. 209 (2014) 172–184.

[26] S. De Gisi, G. Lofrano, M. Grassi, M. Notarnicola, Characteristics and adsorption capacities of low-cost sorbents for wastewater treatment: a review, Sustain. Mater. Technol. 9 (2016) 10–40.

[27] M.S. Sajab, C.H. Chia, S. Zakaria, P.S. Khiew, Cationic and anionic modifications of oil palm empty fruit bunch fibers for the removal of dyes from aqueous solutions, Bioresour. Technol. 128 (2013) 571–577.

[28] O.S. Bello, S. Banjo, Equilibrium, kinetic, and quantum chemical studies on the adsorption of Congo red using Imperata cylindrica leaf powder activated carbon, Toxicol. Environ. Chem. 94 (2012) 1114–1124.

[29] M.A. Ahmad, N. Ahmad, O.S. Bello, Adsorptive removal of malachite green dye using durian seed-based activated carbon, Water, Air. Soil Pollut. 225 (2014) 2057–2076.

[30] M.A. Ahmad, N. Ahmad, O.S. Bello, Modified durian seed as adsorbent for the removal of methyl red dye from aqueous solutions, Appl. Water Sci. 5 (2015) 407–423.

[31] M.A. Ahmad, N. Ahmad, O.S. Bello, Statistical optimization of adsorption process for removal of synthetic dye using watermelon rinds, Model, Earth Syst. Environ. 3 (2017) 1–9.

[32] M.A. Ahmad, N.S. Afandi, O.S. Bello, Optimization of process variables by response surface methodology for malachite green dye removal using lime peel activated carbon, Appl. Water Sci. 7 (2017) 717–727.

[33] O. Üner, Ü. Geçgel, H. Kolancilar, Y. Bayrak, Adsorptive removal of rhodamine B with activated carbon obtained from Okra wastes, Chem. Eng. Commun. 204 (2017) 772–783.

[34] P. Janoš, H. Buchtová, M. Rýznarová, Sorption of dyes from aqueous solutions onto fly ash, Water Res. 37 (2003) 4938–4944.

[35] V.K. Gupta, D. Mohan, S. Sharma, M. Sharma, Removal of basic dyes (rhodamine B and methylene blue) from aqueous solutions using bagasse fly ash, Separ. Sci. Technol. 35 (2000) 2097–2113.

[36] O.S. Bello, O.A. Olusegun, V.O. Njoku, Fly ash: an alternative to powdered activated carbon for the removal of eosin dye from aqueous solutions, Bull. Chem. Soc. Ethiop. 272 (2013) 191–204.

[37] S. Arivoli, Adsorption of rhodamine B by acid activated carbon- thermodynamic and equilibrium studies, Sci. Trans. Enviornment Technovation. 3 (2009) 86–97.

[38] O.S. Bello, M.A. Ahmad, N. Ahmad, Adsorptive features of banana (Musa paradisiaca) stalk-based activated carbon for malachite green dye removal, Chem. Ecol. 28 (2012) 153–167.

[39] A.T. Ojedokun, O.S. Bello, Kinetic modeling of liquid-phase adsorption of Congo red dye using guava leaf-based activated carbon, Appl. Water Sci. 7 (2017) 1965–1977.

[40] B.H. Hameed, A.T.M. Din, A.L. Ahmad, Adsorption of methylene blue onto bamboo-based activated carbon: kinetics and equilibrium studies, J. Hazard. Mater. 141 (2007) 819–825.

[41] S.K. Ghosh, A. Bandyopadhyay, Adsorption of methylene blue onto citric acid treated carbonized bamboo leaves powder: equilibrium, kinetics, thermodynamics analyses, J. Mol. Liq. 248 (2017) 413–424.

[42] V. Gunasekar, V. Ponnusami, Kinetics, equilibrium, and thermodynamic studies on adsorption of methylene blue by carbonized plant leaf powder, J. Chem. (2013) 1–6.

[43] A.L. Cazetta, A.M.M. Vargas, E.M. Nogami, M.H. Kunita, M.R. Guilherme, A.C. Martins, T.L. Silva, J.C.G. Moraes, V.C. Almeida, NaOH-activated carbon of high surface area produced from coconut shell: kinetics and equilibrium studies from the methylene blue adsorption, Chem. Eng. J. 174 (2011) 117–125.

[44] R.A. Rashid, A.H. Jawad, M.A.B.M. Ishak, N.N. Kasim, FeCl 3 -activated carbon developed from coconut leaves: characterization and application for methylene blue removal, Sains Malays. 47 (2018) 603–610.

[45] O.S. Bello, E.S. Owojuyigbe, M.A. Babatunde, F.E. Folaranmi, Sustainable conversion of agro-wastes into useful adsorbents, Appl. Water Sci. 7 (2017) 3561–3571.

[46] B. Cabal, T. Budinova, C.O. Ania, B. Tsyntsarski, J.B. Parra, B. Petrova, Adsorption of naphthalene from aqueous solution on activated carbons obtained from bean pods, J. Hazard. Mater. 161 (2009) 1150–1156.

[47] S.N. Jain, P.R. Gogate, NaOH-treated dead leaves of Ficus racemosa as an efficient biosorbent for Acid Blue 25 removal, Int. J. Environ. Sci. Technol. 14 (2017) 531–542.

[48] S.N. Jain, P.R. Gogate, Adsorptive removal of acid violet 17 dye from wastewater using biosorbent obtained from NaOH and H_2SO_4 activation of fallen leaves of Ficus racemosa, J. Mol. Liq. 243 (2017) 132–143.

[49] S.N. Jain, P.R. Gogate, Acid Blue 113 removal from aqueous solution using novel biosorbent based on NaOH treated and surfactant modified fallen leaves of Prunus Dulcis, J. Environ. Chem. Eng. 5 (2017) 3384–3394.

[50] Z.M. Hussin, N. Talib, N.M. Hussin, M.A.K.M. Hanafiah, W.K.A.W.M. Khalir, Methylene blue adsorption onto NaOH modified durian leaf powder: isotherm and kinetic studies, Am. J. Environ. Eng. 5 (2015) 38–43.

[51] L. Gong, W. Sun, L. Kong, Adsorption of methylene blue by NaOH-modified dead leaves of plane Trees, Comput. Water, Energy, Environ. Eng. 02 (2013) 13–19.

[52] O.S. Bello, K.A. Adegoke, O.O. Akinyunni, Preparation and characterization of a novel adsorbent from Moringa oleifera leaf, Appl. Water Sci. 7 (2017) 1295–1305.

[53] O.S. Bello, B.M. Lasisi, O.J. Adigun, V. Ephraim, Scavenging Rhodamine B dye using moringa oleifera seed pod, Chem. Speciat. Bioavailab. 29 (2017) 120–134.

[54] Y. Tang, Y. Li, Y. Zhao, Q. Zhou, Y. Peng, Enhanced removal of methyl violet using NaOH-modified C. camphora leaves powder and its renewable adsorption, Desalin. Water Treat. 98 (2017) 306–314.

[55] M. Ahmaruzzaman, M.J.K. Ahmed, S. Begum, Remediation of Eriochrome Black T-contaminated aqueous solutions utilizing H 3 PO 4 -modified berry leaves as a non-conventional adsorbent, Desalin. Water Treat. 56 (2015) 1507–1519.

[56] J.X. Yang, G.B. Hong, Adsorption behavior of modified Glossogyne tenuifolia leaves as a potential biosorbent for the removal of dyes, J. Mol. Liq. 252 (2018) 289–295.

[57] C.F. Uzoh, O.D. Onukwuli, J.T. Nwabanne, Characterization, kinetics and statistical screening analysis of gmelina seed oil extraction process, Mater. Renew. Sustain. Energy. 3 (2014) 1–12.

[58] A.A. Inyinbor, F.A. Adekola, G.A. Olatunji, Adsorption of Rhodamine B dye from aqueous solution on Irvingia gabonensis biomass: kinetics and thermodynamics studies, S. Afr. J. Chem. 68 (2015) 115–125.

[59] A.A. Inyinbor, F.A. Adekola, G.A. Olatunji, Kinetics, isotherms and thermodynamic modeling of liquid phase adsorption of Rhodamine B dye onto Raphia hookerie fruit epicarp, Water Resour. Ind. 15 (2016) 14–27.

[60] M.K. Dahri, M.R.R. Kooh, L.B.L. Lim, Remediation of rhodamine B dye from aqueous solution using Casuarina equisetifolia cone powder as a low-cost adsorbent, Adv. Phys. Chem. 2016 (2016) 1–14.

[61] T.A. Khan, S. Sharma, I. Ali, Adsorption of Rhodamine B dye from aqueous solution onto acid activated mango (Magnifera indica) leaf powder: equilibrium, kinetic and thermodynamic studies, J. Toxicol. Environ. Health Sci. 3 (2011) 286–297. http://www.academicjournals.org/article/article1379597780_Khan et al.pdf.

[62] S.L. Hii, S.Y. Yong, C.L. Wong, Removal of rhodamine B from aqueous solution by sorption on Turbinaria conoides (Phaeophyta), J. Appl. Phycol. 21 (2009) 625–631.

[63] M.A. Hossain, M.S. Alam, Adsorption kinetics of Rhodamine-B on used black tea leaves, Iran, J. Environ. Heal. Sci. Eng. 9 (2012) 1.

[64] G. Vijayakumar, R. Tamilarasan, M. Dharmendirakumar, Adsorption, kinetic, equilibrium and thermodynamic studies on the removal of basic dye Rhodamine-B from aqueous solution by the use of natural adsorbent perlite, J. Mater. Environ. Sci. 3 (2012) 157–170.

[65] T.S. Anirudhan, M. Ramachandran, Adsorptive removal of basic dyes from aqueous solutions by surfactant modified bentonite clay (organoclay): kinetic and competitive adsorption isotherm, Process Saf. Environ. Prot. 95 (2015) 215–225.

[66] V. da Silva Lacerda, J.B. López-Sotelo, A. Correa-Guimarães, S. Hernández-Navarro, M. Sánchez-Báscones, L.M. Navas-Gracia, P. Martín-Ramos, J. Martín-Gil, Rhodamine B removal with activated carbons obtained from lignocellulosic waste, J. Environ. Manag. 155 (2015) 67–76.

[67] J.R. Baseri, P.N. Palanisamy, P. Siva Kumar, Adsorption of basic dyes from synthetic textile effluent by activated carbon prepared from Thevetia peruviana, Indian J. Chem. Technol. 19 (2012) 311–321.

[68] M. Mohammadi, A.J. Hassani, A.R. Mohamed, G.D. Najafpour, Removal of rhodamine b from aqueous solution using palm shell-based activated carbon: adsorption and kinetic studies, J. Chem. Eng. Data 55 (2010) 5777–5785.

[69] B.S. Inbaraj, J.T. Chien, G.H. Ho, J. Yang, B.H. Chen, Equilibrium and kinetic studies on sorption of basic dyes by a natural biopolymer poly(γ-glutamic acid), Biochem. Eng. J. 31 (2006) 204–215.

[70] M.R.R. Kooh, M.K. Dahri, L.B.L. Lim, The removal of rhodamine B dye from aqueous solution using Casuarina equisetifolia needles as adsorbent, Cogent Environ. Sci. 2 (2016) 1–14.

[71] H. Lata, V.K. Garg, R.K. Gupta, Adsorptive removal of basic dye by chemically activated Parthenium biomass: equilibrium and kinetic modeling, Desalination 219 (2008) 250–261.

[72] P. Panneerselvam, N. Morad, K.A. Tan, R. Mathiyarasi, Removal of Rhodamine B dye using activated carbon prepared from Palm Kernel Shell and coated with iron oxide nanoparticles, Separ. Sci. Technol. 47 (2012) 742–752.

[73] J. Shah, M. Rasul Jan, A. Haq, Y. Khan, Removal of Rhodamine B from aqueous solutions and wastewater by walnut shells: kinetics, equilibrium and thermodynamics studies, Front. Chem. Sci. Eng. 7 (2013) 428–436.

[74] A. Amalraj, A. Pius, Removal of selected basic dyes using activated carbon from Tannery wastes, Separ. Sci. Technol. 49 (2014) 90–100.

[75] L.B.L. Lim, N. Priyantha, X.Y. Fang, N.A.H. Mohamad Zaidi, Artocarpusodoratissimus peel as a potential adsorbent in environmental remediation to remove toxic Rhodamine B dye, J. Mater. Environ. Sci. 8 (2017) 494–502.

[76] L. Li, S. Liu, T. Zhu, Application of activated carbon derived from scrap tires for adsorption of Rhodamine B, J. Environ. Sci. 22 (2010) 1273–1280.

[77] G. Cinelli, F. Cuomo, L. Ambrosone, M. Colella, A. Ceglie, F. Venditti, F. Lopez, Photocatalytic degradation of a model textile dye using Carbon-doped titanium dioxide and visible light, J. Water Process Eng. 20 (2017) 71–77.

[78] H. Belayachi, B. Bestani, N. Benderdouche, M. Belhakem, The use of TiO2 immobilized into grape marc-based activated carbon for RB-5 Azo dye photocatalytic degradation, Arab. J. Chem. (2015).

[79] Z. Xing, W. Zhou, F. Du, Y. Qu, G. Tian, K. Pan, C. Tian, H. Fu, A floating macro/mesoporous crystalline anatase TiO_2 ceramic with enhanced photocatalytic performance for recalcitrant wastewater degradation, Dalton Trans. 43 (2014) 790–798.

[80] R. Jain, M. Mathur, S. Sikarwar, A. Mittal, Removal of the hazardous dye rhodamine B through photocatalytic and adsorption treatments, J. Environ. Manag. 85 (2007) 956–964.

[81] P.G.T.N. Dhas, H. Gulyas, R. Otterpohl, Impact of powdered activated carbon and anion Exchange resin on photocatalytic treatment of textile wastewater, J. Environ. Prot. (Irvine, Calif). 06 (2015) 191–203.

[82] S. Nethaji, G. Tamilarasan, P. Neehar, A. Sivasamy, Visible light photocatalytic activities of BiOBr-activated carbon (derived from waste polyurethane) composites by hydrothermal process, J. Environ. Chem. Eng. 6 (2018) 3735–3744.

[83] G. Diener, J. Weissbarth, F. Grossmann, R. Schmidt, Obtaining Maxwell's equations heuristically, Am. J. Phys. 81 (2013) 120–123.

[84] A.A. Al-Kahtani, Photocatalytic degradation of rhodamine B dye in wastewater using Gelatin/CuS/PVA nanocomposites under solar light irradiation, J. Biomaterials Nanobiotechnol. 08 (2017) 66–82.

[85] J. Zhao, L. Wang, Degradation of rhodamine B in aqueous solution by the UV/ZnO photocatalytic process, ICMREE2011 - Proc. 2011 Int. Conf. Mater. Renew. Energy Environ. 2 (2011) 1397–1400.

[86] A.A. Ashkarran, E. Mahmoudi, S. Saviz, TiO2nanofibre-assisted photodecomposition of Rhodamine B from aqueous solution, J. Exp. Nanosci. 8 (2013) 678–687.

[87] J.M. Wu, T.W. Zhang, Photodegradation of rhodamine B in water assisted by titania films prepared through a novel procedure, J. Photochem. Photobiol. A Chem. 162 (2004) 171–177.

[88] X. Zheng, D. Li, X. Li, L. Yu, P. Wang, X. Zhang, J. Fang, Y. Shao, Y. Zheng, Photoelectrocatalytic degradation of rhodamine B on TiO2photonic crystals, Phys. Chem. Chem. Phys. 16 (2014) 15299–15306.

[89] J.M. Wu, Photodegradation of rhodamine B in water assisted by titania nanorod thin films subjected to various thermal treatments, Environ. Sci. Technol. 41 (2007) 1723–1728.

[90] H.P. Boehm, Surface oxides on carbon and their analysis: a critical assessment, Carbon N. Y. 40 (2002) 145–149.

[91] M.J.N.R. Ekpete, O.A. Horsfall, Preparation and characterization of activated carbon derived from fluted pumpkin stem waste (Telfairia occidentalis Hook F), Res. J. Chem. Sci. 1 (2011) 10–17.

[92] T.A. Ojo, A.T. Ojedokun, O.S. Bello, Functionalization of powdered walnut shell with orthophosphoric acid for Congo red dye removal, Part. Sci. Technol. 37 (2019) 74–85.

[93] J.C. Cassady, R.E. Johnson, Cognitive test anxiety and academic performance, Contemp. Educ. Psychol. 27 (2002) 270–295.

[94] I. Langmuir, The adsorption of gases on plane surfaces of glass, mica and platinum, J. Am. Chem. Soc. 40 (1918) 1361–1403.

[95] H.M.F. Freundlich, Over the adsorption in solution, J. Phys. Chem. (1906).

[96] V. Temkin, M.J. Pyzhev, Recent modifications to Langmuir isotherms, Acta Physiochim. (1940). URSS.

[97] M.M. Dubinin, The potential theory of adsorption of gases and vapors for adsorbents with energetically nonuniform surfaces, Chem. Rev. 60 (1960) 235–241.

[98] A. Lindgreen, A. Lindgreen, Corruption and unethical behavior: report on a set of Danish guidelines, J. Bus. Ethics 51 (2004) 31–39.

[99] Y.S. Ho, G. McKay, Pseudo-second order model for sorption processes, Process Biochem. 34 (1999) 451–465.

[100] C. Aharoni, M. Ungarish, Kinetics of activated chemisorption. Part 2. - Theoretical models, J. Chem. Soc. Faraday Trans. 1 Phys. Chem. Condens. Phases. 73 (1977) 456–464.

[101] M. Ungarish, C. Aharoni, Kinetics of chemisorption. Deducing kinetic laws from experimental data, J. Chem. Soc. Faraday Trans. 1 Phys. Chem. Condens. Phases. 77 (1981) 975–985.

[102] W.J. Weber, J.C. Morris, Kinetics of adsorption on carbon from solution, J. Sanit. Eng. Div. 89 (1963) 31–60.

[103] O.S. Bello, M.A. Ahmad, Adsorptive removal of a synthetic textile dye using cocoa pod husks, Toxicol. Environ. Chem. 93 (2011) 1298–1308.

[104] O.S. Bello, M.A. Ahmad, Removal of Remazol Brilliant Violet-5R dye using periwinkle shells, Chem. Ecol. 27 (2011) 481–492.

[105] Y. Chun, G. Sheng, G.T. Chiou, B. Xing, Compositions and sorptive properties of crop residue-derived chars, Environ. Sci. Technol. 38 (2004) 4649–4655.

[106] D. Cordell, A. Rosemarin, J.J. Schröder, A.L. Smit, Towards global phosphorus security: a systems framework for phosphorus recovery and reuse options, Chemosphere 84 (2011) 747–758.

[107] N.M. Hilal, A.A. Emam, A.A. El-Bayaa, N.A. Badawy, A.E. Zidan, Adsorption of barium and iron ions from aqueous solutions by the activated carbon produced from mazot ash, Life Sci. J. 10 (2013) 75–83.

[108] O.S. Bello, K.A. Adegoke, O.O. Sarumi, O.S. Lameed, Functionalized locust bean pod (Parkia biglobosa) activated carbon for Rhodamine B dye removal, Heliyon 5 (2019), e02323.

[109] M. Farahani, S.R.S. Abdullah, S. Hosseini, S. Shojaeipour, M. Kashisaz, Adsorption-based cationic dyes using the carbon active sugarcane bagasse, Procedia Environ. Sci. 10 (2011) 203–208.

[110] M.O. Olakunle, A.A. Inyinbor, A.O. Dada, O.S. Bello, Combating dye pollution using cocoa pod husks: a sustainable approach, Int. J. Sustain. Eng. 11 (2018) 4–15.

[111] T. Santhi, S. Manonmani, V.S. Vasantha, Y.T. Chang, A new alternative adsorbent for the removal of cationic dyes from aqueous solution, Arab. J. Chem. 9 (2016) S466–S474.

[112] C.A.P. Almeida, N.A. Debacher, A.J. Downs, L. Cottet, C.A.D. Mello, Removal of methylene blue from colored effluents by adsorption on montmorillonite clay, J. Colloid Interface Sci. 332 (2009) 46–53.

[113] S. Senthilkumaar, P.R. Varadarajan, K. Porkodi, C.V. Subbhuraam, Adsorption of methylene blue onto jute fiber carbon: kinetics and equilibrium studies, J. Colloid Interface Sci. 284 (2005) 78–82.

[114] I. López Arbeloa, P. Ruiz Ojeda, Dimeric states of rhodamine B, Chem. Phys. Lett. 87 (1982) 556–560.

[115] Chuan Lin, J.A. Ritter, B.N. Popov, Correlation of double-layer capacitance with the pore structure of sol-gel derived carbon xerogels, J. Electrochem. Soc. 146 (1999) 3639–3643.

[116] M. Makeswari, T. Santhi, M.R. Ezhilarasi, Adsorption of methylene blue dye by citric acid modified leaves of Ricinus communis from aqueous solutions, J. Chem. Pharm. Res. 8 (2016) 452–462. Available Online: Www.Jocpr.Com.

[117] A.A. Kamaru, N.S. Sani, N.A.N.N. Malek, Raw and surfactant-modified pineapple leaf as adsorbent for removal of methylene blue and methyl orange from aqueous solution, Desalin. Water Treat. 57 (2016) 18836–18850.

[118] E. Olajide Oyelude, U.R. Owusu, Adsorption of Methylene Blue from Aqueous Solution Using Acid Modified Calotropis Procera Leaf Powder, 2011.

[119] M. Goswami, P. Phukan, Enhanced adsorption of cationic dyes using sulfonic acid modified activated carbon, J. Environ. Chem. Eng. 5 (2017) 3508–3517.

[120] H.M.H. Gad, A.A. El-Sayed, Activated carbon from agricultural by-products for the removal of Rhodamine-B from aqueous solution, J. Hazard. Mater. 168 (2009) 1070–1081.

[121] D.L. Postai, C.A. Demarchi, F. Zanatta, D.C.C. Melo, C.A. Rodrigues, Adsorption of rhodamine B and methylene blue dyes using waste of seeds of Aleurites Moluccana, a low cost adsorbent, Alexandria Eng. J. 55 (2016) 1713–1723.

[122] L. Ding, B. Zou, W. Gao, Q. Liu, Z. Wang, Y. Guo, X. Wang, Y. Liu, Adsorption of Rhodamine-B from aqueous solution using treated rice husk-based activated carbon, Colloids Surfaces A Physicochem. Eng. Asp. 446 (2014) 1–7.

[123] S. Dawood, T.K. Sen, Removal of anionic dye Congo red from aqueous solution by raw pine and acid-treated pine cone powder as adsorbent: equilibrium, thermodynamic, kinetics, mechanism and process design, Water Res. 46 (2012) 1933–1946.

[124] X. Yang, B. Al-Duri, Kinetic modeling of liquid-phase adsorption of reactive dyes on activated carbon, J. Colloid Interface Sci. 287 (2005) 25–34.

[125] M.A. Ahmad, R. Alrozi, Removal of malachite green dye from aqueous solution using rambutan peel-based activated carbon: equilibrium, kinetic and thermodynamic studies, Chem. Eng. J. 171 (2011) 510–516.

[126] M. Hema, S. Arivoli, Comparative Study on the Adsorption Kinetics and Thermodynamics of Dyes onto Acid Activated Low Cost Carbon, 2, 2007, pp. 10–17.

[127] J.S. Cao, J.X. Lin, F. Fang, M.T. Zhang, Z.R. Hu, A new absorbent by modifying walnut shell for the removal of anionic dye: kinetic and thermodynamic studies, Bioresour. Technol. 163 (2014) 199–205.

[128] A.T. Ojedokun, O.S. Bello, Liquid phase adsorption of Congo red dye on functionalized corn cobs, J. Dispersion Sci. Technol. 38 (2017) 1285–1294.

[129] R.M. Fitch, in: Th.F. Tadros (Ed.), Polymers in Colloid Systems—Adsorption, Stability and Flow, Elsevier, Amsterdam, 1988, p. 412. J. Polym. Sci. C Polym. Lett. 27 (1989) 505–505.